NANO LETTERS

2008
Vol. 8, No. 8
2535-2540

Facile Synthesis of Bimetallic Nanoplates Consisting of Pd Cores and Pt Shells through Seeded Epitaxial Growth

Byungkwon Lim,[†] Jinguo Wang,[‡] Pedro H. C. Camargo,[†] Majiong Jiang,[§] Moon J. Kim,[‡] and Younan Xia*[,†]

Department of Biomedical Engineering, Washington University, St. Louis, Missouri 63130, Department of Materials Science, University of Texas at Dallas, Richardson, Texas 75083, and Department of Chemistry, Washington University, St. Louis, Missouri 63130

Received June 9, 2008; Revised Manuscript Received June 25, 2008

ABSTRACT

Pd−Pt core−shell nanoplates with hexagonal and triangular shapes were synthesized through the heterogeneous, epitaxial growth of Pt on Pd nanoplates. The Pd nanoplates were synthesized by reducing Na_2PdCl_4 precursor with PVP as a reducing agent, which then served as seeds for the nucleation of Pt atoms formed by reducing H_2PtCl_6 with citric acid. Characterization of the as-prepared Pd−Pt nanoplates by scanning transmission electron microscopy and high-resolution transmission electron microscopy reveals that a thin, uniform Pt shell was formed around the Pd nanoplate, demonstrating the layer-by-layer epitaxial growth of Pt on Pd surface in this approach. The close lattice match between Pd and Pt (lattice mismatch of only 0.77%) and the slow reduction rate associated with the mild reducing power of citric acid play key roles in achieving the epitaxial growth of Pt shells on Pd nanoplates.

Hybridization provides an effective strategy for enhancing the functionality of materials.[1] It is also possible to tune the catalytic, electronic, and optical properties of metal nanoparticles by incorporating a secondary metal on their surfaces.[2] Platinum serves as a major catalyst in many types of reactions due to its exceptional and unique properties as a catalyst for CO oxidation in a catalytic converter, the oxidation and reduction reactions in a fuel cell, nitric acid production, and petroleum cracking.[3] As Pt is extremely expensive, it is highly beneficial to reduce the amount of Pt required in processes where it is essential. In addition, it has been emphasized that the exposure of specific crystal facets that are more intrinsically active for a particular process could improve the efficiency and selectivity of Pt nanocatalysts.[4] It has been shown that deposition of Pt on a Pd single-crystal surface can reduce the material cost while enhancing their catalytic activity. For instance, a Pt monolayer supported on a Pd {111} surface shows an improved activity for oxygen reduction reaction (ORR) relative to pure Pt {111} surface.[5] In addition, it has been shown that the heterointerface between the Pd core and the Pt shell of a Pd−Pt core−shell nanoparticle provides a favorable environment for metal hydride formation, making them useful for hydrogen storage applications.[6]

Heterogeneous epitaxy has long been used in gas-phase deposition to prepare functional heterostructures or junctions.[7] Recently, various bimetallic core−shell nanostructures consisting of noble metals such as Au, Ag, Pd, and Pt have been explored via heterogeneous epitaxial growth in the solution phase, in which preformed nanocrystals served as seeds for the nucleation and growth of a secondary metal with a different chemical identity.[8] To this end, Mirkin and co-workers synthesized triangular Au−Ag core−shell nanoplates by introducing Au and Ag nanoparticles into a photochemical process that converts Ag nanoparticles into nanoplates surrounding the Au cores.[8b] Yang and co-workers used Pt cubes as seeds for conformal growth of Pd cubes, cuboctahedra, and octahedra and for nonconformal anisotropic growth of Au rods.[8c] Tian and co-workers utilized octahedral Au nanocrystals as seeds to induce either epitaxial growth of Ag and Pd cubes or nonepitaxial growth of polycrystalline Pt shells surrounding Au cores.[8d] There are, however, very few reports on the synthesis of binary metallic nanocrystals decorated with thin, uniform Pt shells despite the fact that these nanostructures would be promising for

* Corresponding author, xia@biomed.wustl.edu.
[†] Department of Biomedical Engineering, Washington University.
[‡] Department of Materials Science, University of Texas at Dallas.
[§] Department of Chemistry, Washington University.

10.1021/nl8016434 CCC: $40.75
Published on Web 07/11/2008

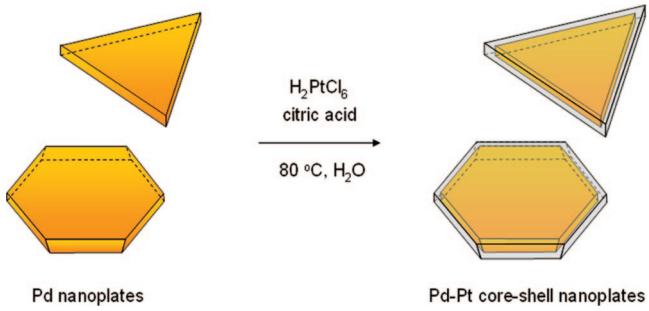

Figure 1. Schematic illustration of the formation of Pd−Pt core−shell nanoplates through epitaxial growth of Pt shells on Pd nanoplates with hexagonal and triangular shapes.

the development of highly active, cost-effective nanocatalysts.

Here we report the facile synthesis of bimetallic nanoplates with the cores being Pd nanoplates and the shells being made of Pt. The Pd nanoplates can have either a hexagonal or triangular shape and can serve as seeds for the nucleation and growth of Pt. Compared to other noble metals, Pd is expected to be well-suited for achieving conformal epitaxial growth of Pt due to a lattice mismatch of only 0.77% between these two metals. More significantly, Pd nanocrystals have recently been prepared in a rich variety of different shapes, making them ideal seeds for shape-controlled synthesis of Pt nanocrystals. Here we demonstrate that the epitaxial growth of Pt on a Pd seed can be achieved from the reduction of a Pt precursor by citric acid in an aqueous solution, leading to the formation of a thin, uniform Pt shell around the Pd nanoplate (Figure 1). Importantly, this work not only provides a novel core−shell nanostructure that has not been accessed by other methods but also opens a new way for the shape-controlled synthesis of binary Pd−Pt core−shell nanocrystals.

The Pd nanoplates were synthesized by reducing Na_2PdCl_4 with poly(vinyl pyrrolidone) (PVP, MW = 55000) in aqueous solutions as reported previously.[9] In a typical procedure, 3 mL of 21.4 mM aqueous Na_2PdCl_4 solution was added to 8 mL of 0.08 mM aqueous PVP solution and heated at 80 °C in air under magnetic stirring for 24 h. The molar ratio of the repeating unit of PVP to the Pd precursor was 5:1. Figure 2 shows transmission electron microscopy (TEM) and scanning electron microscopy (SEM) images of the resulting Pd nanoplates. The sample contained both hexagonal and triangular nanoplates with edge lengths in the range of 50−100 nm. The thickness of the nanoplates was measured to be 24 ± 2 nm. The Pd nanoplates exhibit sharp edges and corners as well as smooth surfaces. The electron diffraction (ED) pattern taken from the Pd nanoplate is composed of diffraction spots with a 6-fold rotational symmetry (see the inset of Figure 2A), indicating that the top and bottom faces of the Pd nanoplate are enclosed by the {111} planes.

The Pd−Pt core−shell nanoplates were synthesized by reducing H_2PtCl_6 with citric acid in the presence of the Pd nanoplates as seeds and PVP as a stabilizing agent in an aqueous solution, respectively. In a typical experiment, 6 mL

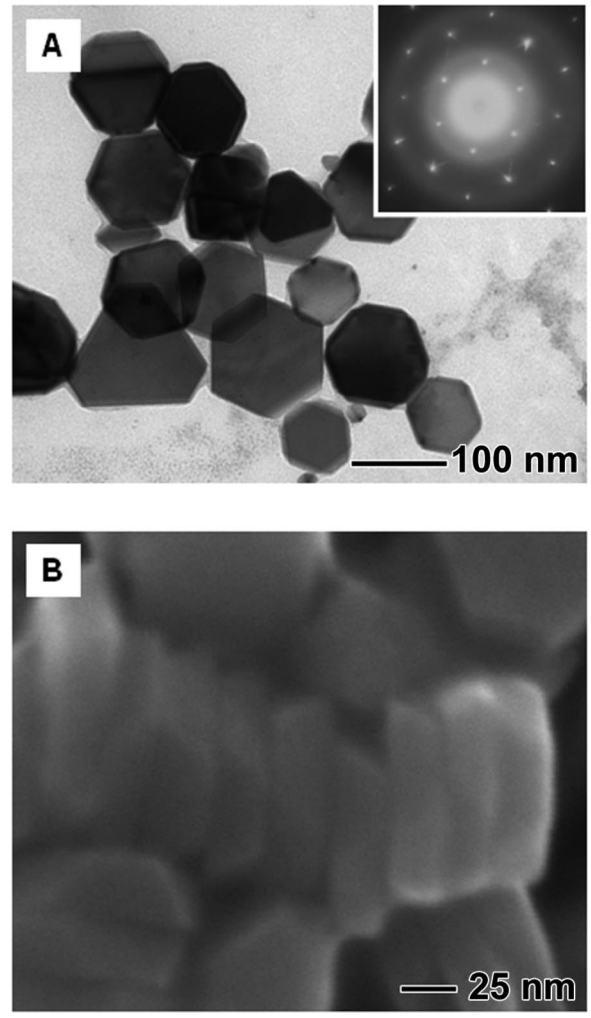

Figure 2. (A) TEM and (B) SEM images of Pd nanoplates synthesized by reducing the Na_2PdCl_4 precursor with PVP. The molar ratio of the repeating unit of PVP to the Pd precursor was 5:1. Inset of (A) gives the corresponding electron diffraction pattern, showing that the top and bottom faces of the Pd nanoplates are bounded by {111} planes.

of an aqueous solution containing H_2PtCl_6 (10.7 mM), citric acid (52.0 mM), and PVP (0.11 mM in terms of the repeating unit) was mixed with 4 mL of the as-prepared Pd nanoplate solution and heated to 80 °C in air under magnetic stirring for 5 h. After the reaction, the product was collected by centrifugation. The TEM image of the product shows that the nanoplates tended to stack and lie on the TEM grid against one of their side faces rather than the top and bottom faces (Figure 3A). The thickness of the product was estimated to be 28 ± 2 nm. The high-resolution TEM (HRTEM) study reveals that there are {111} twin planes parallel to the top and bottom faces of the nanoplates (Figure 3B). The SEM image clearly shows that the product retains the morphologies of hexagonal and triangular plates as well as the smooth surface (Figure 3C). Both TEM and SEM images show the absence of isolated Pt nanoparticles. The SEM/EDX analysis indicates that the weight percentage for Pt in the product was 14% (Figure 3D).

We performed scanning transmission electron microscopy (STEM) and EDX line scanning analyses to reveal the

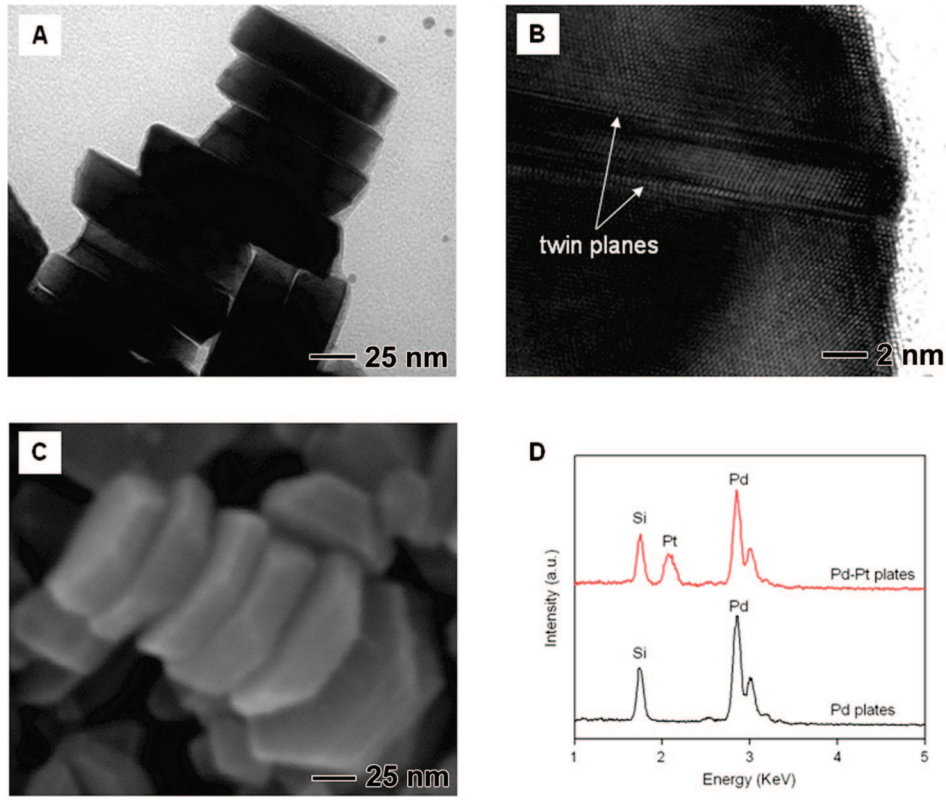

Figure 3. (A) TEM and (B) HRTEM images taken from the side faces of Pd−Pt nanoplates. In (B), it can be clearly seen that there are {111} twin planes parallel to the top and bottom faces of the nanoplate. (C) SEM image of the Pd−Pt nanoplates. (D) EDX spectra taken from the Pd and Pd−Pt nanoplates, respectively.

compositional variation over the Pd−Pt nanoplate. The STEM image and the compositional line profile taken from the top face of a single hexagonal nanoplate indicate that Pt atoms were deposited on the flat top and bottom faces, as well as the side faces of the Pd hexagonal nanoplate (Figure 4A,B). The STEM image and three compositional line profiles on a single triangular nanoplate also confirm the deposition of Pt atoms on the entire surface of the triangular nanoplate (Figure 4C−F). These results demonstrate the successful preparation of the core−shell nanostructure consisting of the Pd nanoplate as a core and a complete shell of Pt.

We also investigated the compositional variation along the side faces of the Pd−Pt nanoplate. As shown in the STEM image (Figure 5A), the Pt layers that cover the top and bottom faces of the Pd nanoplate exhibit much higher intensity than the Pd core due to the enhanced contrast from the difference in atomic numbers between Pd and Pt. We can see that the Pt shells are very thin, on the scale of 1−2 nm. The compositional line profile along the side faces of nanoplates also shows a core−shell structure for the Pd−Pt nanoplates (Figure 5B). The HRTEM images taken from the side faces of the nanoplates reveal the continuous lattice fringes from the Pd core to the Pt shell (Figure 5C,D). The lattice spacings between neighboring fringes in Pd and Pt regions are measured to be 2.22 and 2.29 Å, respectively. These values are in good agreement with the distances between two adjacent {111} planes of face-centered cubic (fcc) Pd (2.25 Å) and Pt (2.27 Å). These results demonstrate the development of the conformal Pt shell through the layer-by-layer epitaxial growth of Pt on Pd {111} surfaces.

Figure 6 represents the HRTEM images taken along a direction perpendicular to the top faces of the hexagonal and triangular Pd−Pt nanoplates. Both the hexagonal and triangular nanoplates exhibited the flat {111} surfaces with a lattice spacing of 1.39 Å, which can be indexed as {220} of Pt. The corresponding Fourier transform (FT) patterns give arrays of spots with a 6-fold rotational symmetry in both cases, which can be indexed to the {220} reflections (insets of panels B and D). These results indicate that the top and bottom faces of the nanoplates are enclosed by the Pt {111} surfaces and also that the added Pt atoms continue with the same crystal structure as the underlying Pd core.

As demonstrated in the syntheses of Pt−Pd and Au−Ag binary nanocrystals, the close lattice match between the seed and the deposited atoms plays a critical role in achieving the conformal epitaxial growth of the second metal.[8c,d,10] When there is a large lattice mismatch between the seed and the deposited atoms, heterogeneous epitaxial growth is not favorable due to high strain energy as in the case of the Au−Pt binary system.[8d] Since a lattice mismatch between Pd and Pt is very small (only 0.77%), Pd nanocrystals can be considered as an ideal platform for the epitaxial growth of Pt shells. It is also worth emphasizing that the slow reduction rate associated with the mild reducing power of citric acid also plays an significant role in the conformal growth of Pt shells on Pd nanoplates.[11] Yang and co-workers have recently reported that in the synthesis of Pt−Pd binary

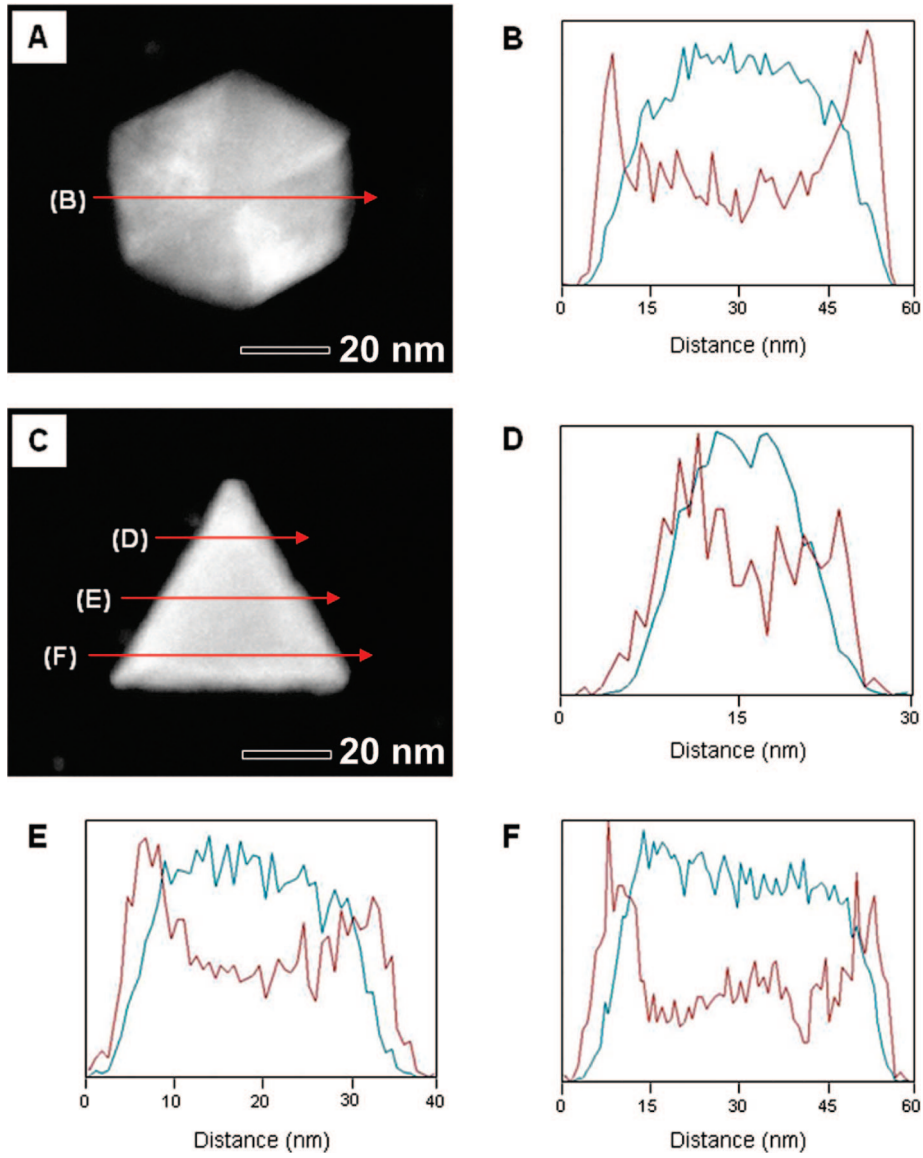

Figure 4. (A) STEM image and (B) cross-sectional compositional line profile of a Pd−Pt core−shell nanoplate with a hexagonal shape. (C) STEM image and (D−F) cross-sectional compositional line profiles of a Pd−Pt core−shell nanoplate with a triangular shape. In the composition line profiles, blue and red represent Pd and Pt, respectively.

nanocrystals from cubic Pt seeds the increase of reduction rate led to multiple nucleation of Pd primarily on the corners of cubic Pt seeds rather than the conformal epitaxial growth of thin Pd shells despite their small lattice mismatch.[12] In the present work, we believe that both the close lattice match between Pd and Pt and the slow reduction rate associated with the mild reducing power of citric acid play crucial roles in achieving the layer-by-layer epitaxial growth of Pt shells on Pd nanoplates.

As we and others have demonstrated for the Ag system, the crystallinity of a seed plays a key role in determining the final shape of a nanocrystal.[13] In contrast to the other noble metals such as Au, Ag, and Pd, twinned structures such as plates, icosahedra, and decahedra are rarely found in Pt nanocrystals probably due to the high internal strain energy associated with Pt twinned seeds.[14] Among all noble metals, we and other groups have demonstrated probably the largest number of shapes for Pd.[9,11,15] The successful preparation of Pd−Pt core−shell nanoplates through the epitaxial growth of Pt on Pd surfaces suggests that the methodology established for this Pd−Pt system could be easily extended to generate various single-crystal and twinned Pd−Pt binary nanocrystals by taking advantage of the wide range of shapes for Pd nanocrystals.

In summary, we have demonstrated the synthesis of a new type of hybrid nanostructure in the platelike morphology consisting of a Pd core and a Pt shell. The formation of such morphology involved the heterogeneous, epitaxial growth of Pt on Pd nanoplate seeds. STEM/EDS and HRTEM analyses revealed the formation of a thin Pt shell on the entire surface of a Pd nanoplate through conformal epitaxial growth mode. It is expected that these Pd−Pt nanoplates, combining the properties from both Pd and Pt, may find use in many applications including catalytic oxidation, oxygen reduction, and hydrogenation and hydrogen storage.

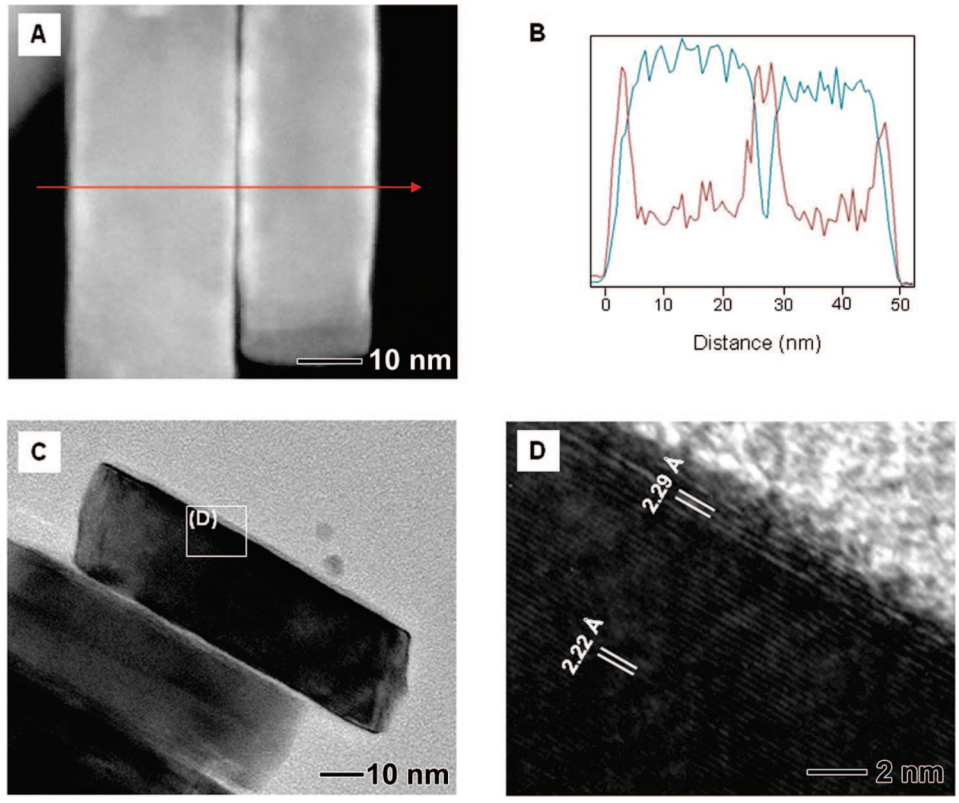

Figure 5. (A) STEM image and (B) cross-sectional compositional line profile taken from the side faces of the Pd−Pt core−shell nanoplates (Pd, blue; Pt, red). (C, D) HRTEM images of the nanoplates, which show the continuous lattice fringes from the Pd core (lattice spacing 2.22 Å) to the Pt shell (lattice spacing 2.29 Å).

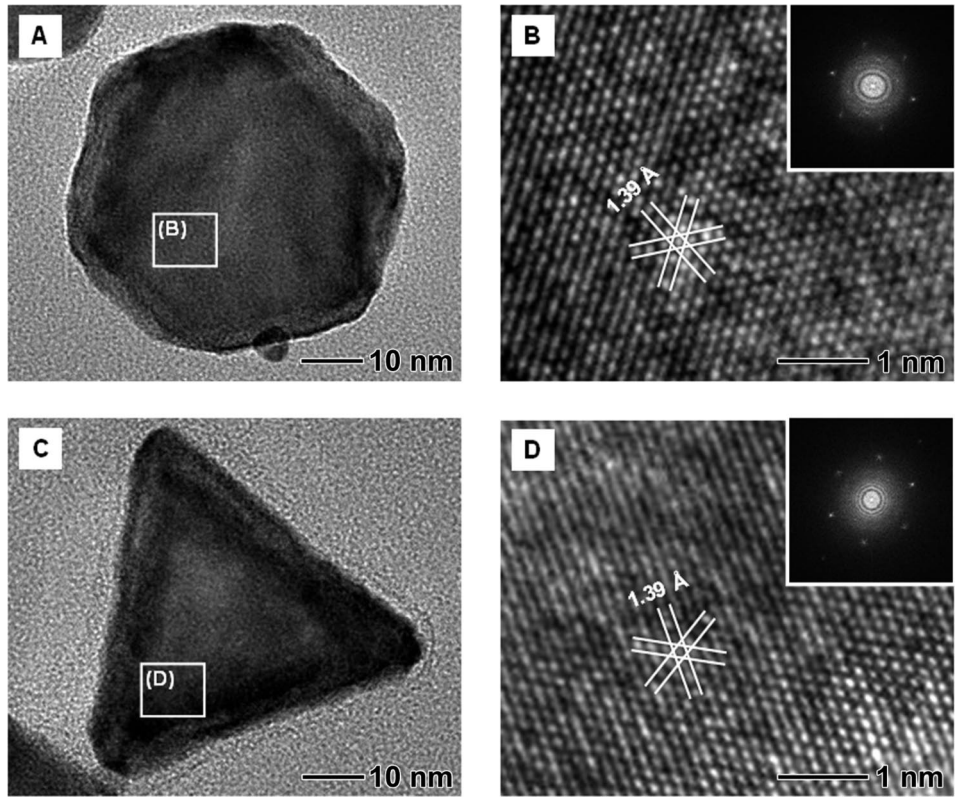

Figure 6. HRTEM images taken along a direction perpendicular to the flat top faces of (A, B) hexagonal and (C, D) triangular Pd−Pt core−shell nanoplates. The lattice spacings of 1.39 Å can be indexed as {220} of Pt, indicating that the top and bottom faces are enclosed by the Pt {111} planes. The corresponding FT patterns show a 6-fold hexagonal symmetry (insets), which can be indexed to the {220} reflections.

Acknowledgment. This work was supported in part by ACS-PRF (44353-AC10) and the NSF (both DMR-0451788 and DMR-0804088), as well as a Director's Pioneer Award from the NIH (5DPOD000798). B.L. was also partially supported by the Postdoctoral Fellowship Program of the Korea Research Foundation. J.W. was supported by a grant from CNMT-MOST (No. M105KO010026-05K1501-02611).

References

(1) (a) Gao, J. H.; Liang, G. L.; Zhang, B.; Kuang, Y.; Zhang, X. X.; Xu, B. *J. Am. Chem. Soc.* **2007**, *129*, 1428. (b) Gao, J. H.; Zhang, B.; Gao, Y.; Pan, Y.; Zhang, X. X.; Xu, B. *J. Am. Chem. Soc.* **2007**, *129*, 11928. (c) Maksimuk, S.; Yang, S. C.; Peng, Z. M.; Yang, H. *J. Am. Chem. Soc.* **2007**, *129*, 8694. (d) Camargo, P. H. C.; Xiong, Y.; Ji, L.; Zuo, J. M.; Xia, Y. *J. Am. Chem. Soc.* **2007**, *129*, 15452.

(2) (a) Chen, M.; Kumar, D.; Yi, C.-W.; Goodman, D. W. *Science* **2005**, *310*, 291. (b) Enache, D. I.; Edwards, J. K.; Landon, P.; Solsona-Espriu, B.; Carley, A. F.; Herzing, A. A.; Watanabe, M.; Kiely, C. J.; Knight, D. W.; Hutchings, G. J. *Science* **2006**, *311*, 362. (c) Zhang, J.; Sasaki, K.; Sutter, E.; Adzic, R. R. *Science* **2007**, *315*, 220.

(3) Ertl, G. *Handbook of Heterogeneous Catalysis*, Wiley-VCH: Weinheim, 2008.

(4) Bratlie, K. M.; Lee, H.; Komvopoulos, K.; Yang, P.; Somorjai, G. A. *Nano Lett.* **2007**, *7*, 3097.

(5) Zhang, J.; Vukmirovic, M. B.; Xu, Y.; Mavrikakis, M.; Adzic, R. R. *Angew. Chem., Int. Ed.* **2005**, *44*, 2132.

(6) Kobayashi, H.; Yamauchi, M.; Kitagawa, H.; Kubota, Y.; Kato, K.; Takata, M. *J. Am. Chem. Soc.* **2008**, *130*, 1818.

(7) (a) Chambers, S. A. *Adv. Phys.* **1991**, *40*, 357. (b) Ledentsov, N. N.; Ustinov, V. M.; Shchulan, V. A.; Kop'er, P. S.; Alferov, Zh. I.; Bimbers, D. *Semiconductors* **1998**, *32*, 343.

(8) (a) Xiang, Y.; Wu, X.; Liu, D.; Jiang, X.; Chu, X.; Li, Z.; Ma, L.; Zhou, W.; Xie, S. *Nano Lett.* **2006**, *6*, 2290. (b) Xue, C.; Millstone, J. E.; Li, S.; Mirkin, C. A. *Angew. Chem., Int. Ed.* **2007**, *46*, 8436. (c) Habas, S. E.; Lee, H.; Radmilovic, V.; Somorjai, G. A.; Yang, P. *Nat. Mater.* **2007**, *6*, 692. (d) Fan, F.-R.; Liu, D.-Y.; Wu, Y.-F.; Duan, S.; Xie, Z.-X.; Jiang, Z.-Y.; Tian, Z.-Q. *J. Am. Chem. Soc.* **2008**, *130*, 6949.

(9) Xiong, Y.; Washio, I.; Chen, J.; Cai, H.; Li, Z.-Y.; Xia, Y. *Langmuir* **2006**, *22*, 8563.

(10) Seo, D.; Yoo, C. I.; Jung, J.; Song, H. *J. Am. Chem. Soc.* **2008**, *130*, 2940.

(11) (a) Xiong, Y.; Washio, I.; Chen, J.; Sadilek, M.; Xia, Y. *Angew. Chem., Int. Ed.* **2007**, *46*, 4917. (b) Lim, B.; Xiong, Y.; Xia, Y. *Angew. Chem., Int. Ed.* **2007**, *46*, 9279.

(12) Lee, H.; Habas, S. E.; Somorjai, G. A.; Yang, P. *J. Am. Chem. Soc.* **2008**, *130*, 5406.

(13) (a) Wiley, B.; Sun, Y.; Mayers, B.; Xia, Y. *Chem. Eur. J.* **2005**, *11*, 454. (b) Wiley, B.; Sun, Y.; Chen, J.; Cang, H.; Li, Z.-Y.; Li, X.; Xia, Y. *MRS Bull.* **2005**, *30*, 356. (c) Wiley, B.; Im, S.-H.; Li, Z.-Y.; McLellan, J. M.; Siekkinen, A.; Xia, Y. *J. Phys. Chem. B* **2006**, *110*, 15666.

(14) (a) Chen, J.; Herricks, T.; Geissler, M.; Xia, Y. *J. Am. Chem. Soc.* **2004**, *126*, 10854. (b) Chen, J.; Herricks, T.; Xia, Y. *Angew. Chem., Int. Ed.* **2005**, *44*, 2.

(15) (a) Xiong, Y.; Chen, J.; Wiley, B.; Xia, Y.; Aloni, S.; Yin, Y. *J. Am. Chem. Soc.* **2005**, *127*, 7332. (b) Xiong, Y.; Cai, H.; Wiley, B. J.; Wang, J.; Kim, M. J.; Xia, Y. *J. Am. Chem. Soc.* **2007**, *129*, 3665. (c) Xiong, Y.; Cai, H.; Yin, Y.; Xia, Y. *Chem. Phys. Lett.* **2007**, *440*, 273. (d) Xiong, Y.; Xia, Y. *Adv. Mater.* **2007**, *19*, 3385.

NL8016434